Technology in Cancer Research and Treatment
ISSN 1533-0346
Volume 13, Number 6, December 2014

Evaluation of Image-guidance Strategies for Prostate Cancer

www.tcrt.org
DOI: 10.7785/tcrt.2013.600258

T. Piotrowski, Ph.D.[1,2]*
K. Kaczmarek, M.Sc.[3]
T. Bajon, M.D.[3]
A. Ryczkowski, M.Sc.[2]
A. Jodda, M.Sc.[2]
J. Kaźmierska, M.D., Ph.D.[1,3]

[1]Department of Electroradiology, University of Medical Sciences, Poznan, Poland
[2]Department of Medical Physics, Greater Poland Cancer Centre, Poznan, Poland
[3]2nd Radiotherapy Department, Greater Poland Cancer Centre, Poznan, Poland

In this study, set-up accuracy and time consumption of different image-guidance protocols used for prostate cancer patients were compared. Set-up corrections from 60 prostate cancer patients treated on helical tomotherapy (HT) were used to simulate four types of image-guidance protocols which were based on: (i) a limited number of imaging sessions (IG-1), (ii) reduced registration tasks during daily imaging (IG-2), or (iii) and (iv) mixed methods of imaging (IG-3, IG-4). Each protocol was evaluated for three referencing scenarios based on the first fraction, first three fractions and first five fractions. Residual set-up error, the difference between the average set-up correction and the actual correction required, was used to evaluate the accuracy of each protocol. The first five fractions referencing scenario provides the highest reduction of the margins for each image-guidance protocol evaluated in this study. The first type of protocol is the shortest way to the effective correction of the systematic component of set-up error. For the second type of the protocol, the control of the residual errors is better and, as a result, the reduction of the margins is more significant than that obtained for the first one. Moreover, the second type of the protocol provides the highest accuracy of delivered dose. The result obtained for the fourth type of protocol does not decrease the calculated margins or increase their accuracy in correspondence to the no image guidance scheme. The fourth type of the protocol is not recommended as a protocol to be used to increase the conformity of the dose. The choice of the rest protocols should be validated in the context of (i) institutional practice regarding patient set-up procedure and its time consumption, (ii) acceptable balance between the amount of the dose delivered to the organ at risk and the additional imaging dose and (iii) patient anatomical conditions.

Key words: Helical tomotherapy; Image guided radiation therapy; Margins; Megavoltage CT; Cone beam CT; Prostate cancer.

Introduction

The intensity modulated radiation therapy (IMRT) applied for treatments of prostate cancers allows for delivering dose to the target with the higher-dose gradient around the target than the three dimensional radiation therapy (1, 2). Therefore,

Abbreviations: IMRT: Intensity Modulated Radiation Therapy; IG: Image Guidance; PTV: Planning Target Volume; CT: Computed Tomography; HT: Helical Tomotherapy; kVCT: Kilo-voltage Computed Tomography; LR: Left-right; SI: Superior-inferior; AP: Anterior-posterior; EBRT: External Beam Radiation Therapy; MVCT: Mega-voltage Computed Tomography; TS: Total Shift; AR: Automatic Registration; B: Bone; ST: Soft Tissue; MC: Manual Correction; RE: Residual Errors; ATS: Average of the Total Shifts; AMC: Average of the Manual Corrections; AST: Average Calculated from the Sum of the Manual Corrections and Automatic Registrations based on the Soft Tissues; AAB: Average of the Automatic Registration based on the Bones; R: Referencing Scenario; NIG: No Image Guidance; Σ: Systematic Error; SD: Standard Deviation; σ: Random Population Error; N: Number of the Failed Observation.

*Corresponding author:
Tomasz Piotrowski, Ph.D.
Phone: +48 618850763
E-mail: tomasz.piotrowski@me.com

a proper use of the IMRT demands consistent and accurate localisation of the prostate before treatment delivery (3-5).

Set-up uncertainties during the treatment planning and delivery processes can lead to a geographic miss of the prostate (6). Daily set-up errors are composed of systematic and random components. The systematic component is a deviation that occurs in the same direction and is of a similar magnitude for each fraction throughout the treatment course. The random component is a deviation that can vary in direction and magnitude for each delivered treatment fraction (7).

The use of image guidance (IG) platforms for in-room detection and correction of set-up errors offers the opportunity to reduce margins (6, 7). However, as always, there is an associated cost of increased total time for the treatment, additional radiation dose for imaging, and more workload. There are several publications investigating a proper balance between cost and benefit for prostate cancer patients with a possibility for reduced IG. The M. D. Anderson group (8, 9) conducted an interesting retrospective study of the residual localization errors with different imaging scenarios and the London group proposed to use a limited number of imaging procedures during a couple of initial treatment fractions for establishing the personalized planning target volume (PTV) margins for the rest of the treatment (10-12). These investigations considered two extreme options: either to perform pre-treatment imaging or not. But in practice, the IG process is performed in two steps: (i) patient positioning on the external marks (tattoos), computed tomography (CT) scan, automatic fusion (registration) of the planning CT with the just acquired image followed by (ii) an inspection by the radiation therapists of the resulting match as per instructions of the treating physician and manual correction shifts.

The purpose of this retrospective study was to evaluate: (i) IG protocols that use set-up error information collected over an initial number of treatment fractions to determine an appropriate average set-up correction that could be applied to subsequent fractions and (ii) IG protocols which use set-up error information from the reduced daily registration tasks, performed during the whole course of the radiation therapy. The evaluation was performed with a special emphasis on the accuracy of dose delivery, size of the margins, which should be applied according to a selected IG protocol and time-consumption of the IG protocols.

Material and Methods

The study included 60 patients diagnosed with locally advanced prostate cancer radically treated with a helical tomotherapy (HT) (Accuray Inc., Sunnyvale, CA, USA) between July 2009 and September 2011 at the 2nd Radiotherapy Department of the Greater Poland Cancer Centre, Poznan, Poland. The group of the patients evaluated in this study was described by Bajon *et al.* (13).

For treatment planning, a kilo-voltage computed tomography (kVCT) scans with a 3 mm slice thickness of the pelvis was acquired with a Siemens Sensation Open CT scanner (Siemens AG, Erlangen, Germany). The patients treated in a prone position were immobilised using a belly board immobilization device (Civco Meddical Solutions, Kalona, IA, USA) and feet fixations (14). The combifix immobilization device (Civco Medical Solutions, Kalona, IA, USA) was used for patients treated in a supine position. All patients were asked to empty their bladder and drink 500 ml of water one hour before the scanning procedure on the CT and try to empty their rectum. Following the kVCT scans acquisition, set-up tattoos were marked on the skin. Using the Eclipse 7.3.10 (Varian Medical Systems Inc., Palo Alto, CA, USA), the clinical target volumes (prostate and seminal vesicles) and the organ at risks (rectum, bladder and femurs) were contoured. Margins of 10 mm were applied in the left-right (LR), superior-inferior (SI) and anterior directions, and 7 mm in the posterior direction to create a PTV. After creating all necessary structures, kVCT scans as well as contours were exported in DICOM format to the Hi-Art Tomotherapy planning system (Accuray Inc., Sunnyvale, CA, USA).

All patients had 25 fractions (up to 50 Gy for prostate and seminal vesicles) of external beam radiation therapy (EBRT) followed by a brachytherapy boost (15-17). The dose was prescribed and normalized following recommendations from the report number 83 of the International Commission on Radiation Units and Measurements (18). For every patient, the EBRT plans were prepared in two positions. Based on the comparative analysis of dose distribution, the better plan was selected by a radiation oncologist for realisation on the HT (13). Finally, twenty-nine patients were treated in a prone and thirty-one in a supine position. Typical parameters used for EBRT were: 2.5 cm field width, 0.287 pitch, and modulation factor ranged from 2.5 to 2.8 (19, 20).

For each patient, a daily mega-voltage computed tomography (MVCT) scans with a 4-mm inter-slice distance were acquired prior to the daily treatment. The daily MVCT scans were co-registered automatically with the planning kVCT scans using a mutual information algorithm using the "Bone and Soft Tissue" technique (21). After visual inspection of the automatic registration, additional, manual corrections were performed to increase the reduction of the differences between the planned (kVCT scans) and actual (daily MVCT scans) position of the prostate. The attending radiation oncologist reviewed the quality of the registration during the first imaging session.

The data of 1500 daily shifts were used for margin calculation, which were adequate for four different schemes of IG

protocols: IG-1 based on limited number of imaging sessions, IG-2 based on the reduced registration tasks during daily imaging, IG-3 simulating the scheme when cone-beam CT for the initial fractions is followed by portal imaging for the rest of the fractions and IG-4 simulating the scheme when only limited number of sessions based on portal imaging was used (Figure 1). Moreover, time needed for IG procedures was calculated for each IG scheme.

Total shift in each of the directions along the *x*, *y* or *z*-axis is a sum of shifts resulting from automatic registration and manual correction. In the majority of tomotherapy centres, the procedures of IG assume that automatic registration is performed in the "Bone and Soft Tissues" technique (8, 10-12, 22, 23). In this case, the formula for the total shift becomes as follows:

$$TS_i = AR_i^{B,ST} + MC_i \quad [1]$$

where TS is a total shift, i is one of the possible directions along the *x*, *y* or *z*-axis, AR is an automatic registration performed by the "Bone and Soft Tissues" (B,ST) technique and MC is a manual correction performed after visual inspection of the automatic registration.

However, HT offers also another interesting kind of automatic registration – the "Bone" technique, which registers the MVCT scans with the kVCT scans only on the basis of bone anatomy. Therefore, $AR_i^{B,ST}$ could be described as:

$$AR_i^{B,ST} = AR_i^{B} + AR_i^{ST} \quad [2]$$

where AR_i^{B} is an automatic registration performed by the "Bone" technique and AR_i^{ST} is an component of the $AR_i^{B,ST}$ including information about shifts caused by whole soft tissues, and defined as a difference between the "Bone and Soft Tissues" technique and the "Bone" technique ($AR_i^{B,ST} - AR_i^{B}$).

The TS_i components, resulting from the "Bone and Soft Tissues" registration technique ($AR_i^{B,ST}$) and manual corrections (MC_i) were collected and recorded prospectively for each patient, each time before delivering fraction dose. In order to obtain the TS component based on the "Bone"

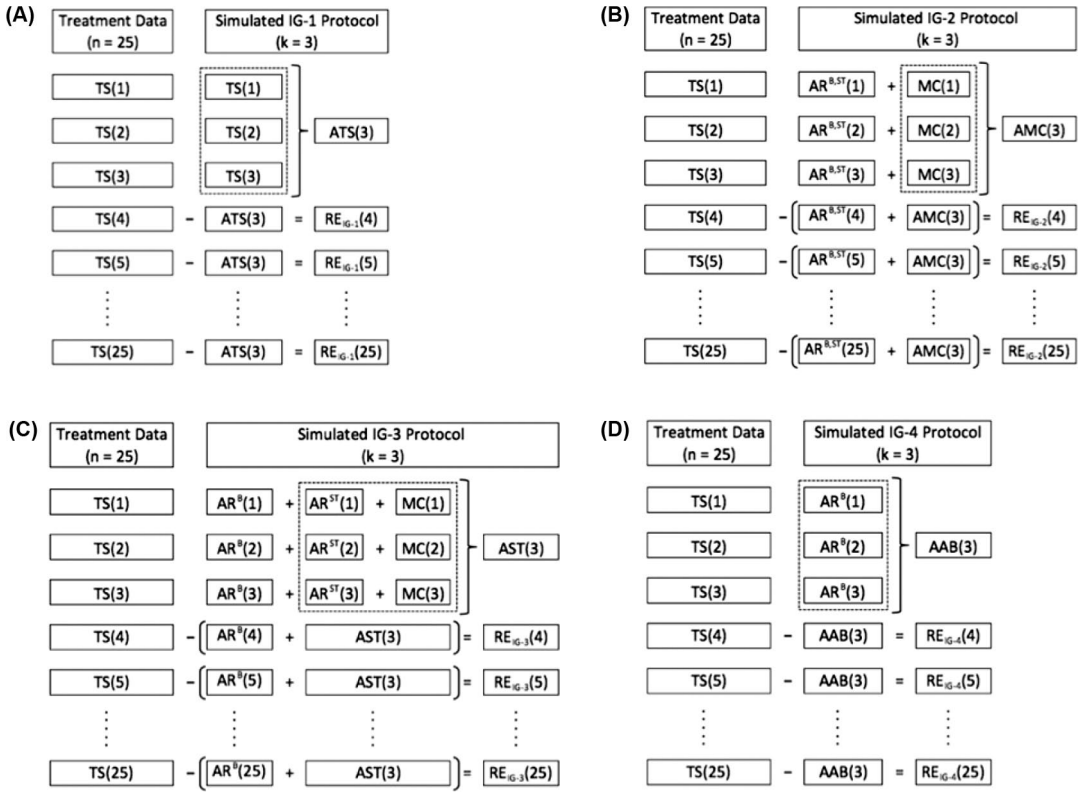

Figure 1: Schemes of the image guidance (IG) protocols used in the study: (**A**) IG-1, (**B**) IG-2, (**C**) IG-3 and (**D**) IG-4 which were based on the referencing scenario including the first three fractions as a reference (R3). Meaning of abbreviations used: n: number of the fraction; k: number of the initial fractions used as a reference; TS: total shift; AR^{B}: automatic registration based on the bony anatomy; $AR^{B,ST}$: full automatic registration; AR^{ST}: automatic registration based on the anatomy of soft tissues; MC: manual correction; RE: residual errors; ATS, AMC, AST and AAB: averages of the total shifts collected during the first three fractions ($k = 3$) for the IG-1, IG-2, IG-3 and IG-4 protocol.

technique (AR_i^B), additional automatic registration was performed using Planned Adaptive software (Accuray Inc., Sunnyvale, CA, USA).

For each patient, the TS_i components from the daily IG history were used to simulate four types of IG protocols (IG-1, IG-2, IG-3, IG-4).

The first of them was based on the methodology presented by Yeung *et al.* (12), which implies reduced numbers of imaging sessions. For this type of protocol (IG-1), we assumed that IG was performed for an initial number of k (1, 2, 3, . . . , k) fractions and that IG was discontinued after the k-th fraction. The average of the TS_i from k fractions ($ATS_i(k)$) was considered as a correction to be applied to subsequent treatment fractions when IG was discontinued. The differences between the TS_i for each j-th fraction ranged from $k+1$ fraction to the last n fraction and the $ATS_i(k)$ were defined as residual fraction errors $RE_{IG\text{-}1}(j)$.

The second type of protocol (IG-2) was proposed by the authors of the present article. It differs from the previous one in that the components of the TS_i were recorded separately during initial k fractions while the average was calculated only basing on manual corrections ($AMC_i(k)$). For the remaining n-k fractions, IG is reduced to automatic registration using the "Bone and Soft Tissues" ($AR_i^{B,ST}$) and $AMC_i(k)$ was considered as a correction. As a result, residual fraction errors $RE_{IG\text{-}2}(j)$ were designated as differences between manual corrections applied for j-th fraction from the range from $k+1$ to n and $AMC_i(k)$.

The third and the fourth protocols (IG-3, IG-4) were based on the methodology presented by Snir *et al.* (24) and were constructed for simulations of the scenarios where different or mixed methods of imaging were used. The IG-3 included full IG procedures for initial k fractions as in IG-1 and IG-2 protocols. The average was calculated from the sum of the AR_i^{ST} and the $MC_i(AST_i(k))$ and was used as a correction for the rest of the n-k fractions, which were supplemented by IG reduced to automatic registration using the "Bone" technique (AR_i^B). Residual fraction errors $RE_{IG\text{-}3}(j)$ for this protocol were defined as a difference between shifts of the soft tissues including prostate for j-th fraction and $AST_i(k)$.

The IG-4 simulated a situation when initial k fractions were controlled only by the automatic registration based on the bone anatomy. The average of the AR_i^B from k fractions ($AAB_i(k)$) was considered as a correction to be applied to subsequent treatment fractions when IG was discontinued. Residual fraction errors $RE_{IG\text{-}4}(j)$ were defined as a difference between the total shifts for j-th fraction and $AAB_i(k)$.

For each protocol, three referencing scenarios (R1, R3 and R5) were analysed. R1 included as the initial fractions only the first fraction ($k = 1$), R3 – the first three fractions ($k = 3$) and R5 – the first five fractions ($k = 5$). Consequently, we analysed twelve scenarios (three scenarios for each protocol) (25-27).

All IG protocols (IG-1, IG-2, IG-3, IG-4) were analysed in the light of the situation where no image guidance (NIG) was used, and the applied margins were calculated on the institutional experience based on the data from daily IG procedure.

The treatment margin required to encompass residual set-up errors for each simulated IG protocol was calculated using the van Herk formula ($2.5\Sigma + 0.7\sigma$), a well known population-based method of determining the margin that could ensure a minimum of 95% dose coverage for 90% of patients (28).

The systematic population error (Σ) was defined as an indication of the spread of individual mean residual errors. It is calculated as the standard deviation (SD) of the distribution of mean residual errors for each individual patient. The random population error (σ) was calculated as the mean of individual random errors. Individual random errors for each patient from the population were defined as the standard deviation (SD) of the measured residual errors over the course of treatment and quantified the spread of residual errors (7).

The variable N, defined as a failed observation, was used in this study to evaluate the distribution of the shifts recorded during the fractions which were higher than the margin applied according to the selected IG protocol. During every fraction three shifts along the LR, SI and anterior-posterior (AP) direction were recorded. If one of them was higher than the applied margin, the fraction was classified as N.

To evaluate the implications on daily workload and the scheduling of patients according to the IG-1, IG-2, IG-3 and IG-4 protocols, time analyses for each component of the overall treatment time such as positioning, imaging, registration, and irradiation, were performed. A detailed analysis included: (i) overall scanning time for each patient according to the protocol; (ii) time needed for each type of the automatic registrations; (iii) time needed for manual corrections. The analysis was performed retrospectively using archived patient data by the in-house software (29, 30).

Statistical analysis was performed in two steps. First, the differences of the residual errors obtained for groups divided by the referencing scenarios (R1, R3 and R5) were analyzed

for each IG protocol separately. Based on these results, the best referencing scenario was selected for each IG protocol and then used for analysis of the differences between IG protocols.

In each situation non-parametric analysis of variance for dependent samples (Friedman ANOVA) was performed. In situation when statistically significant differences between variances of the analysed groups were confirmed, additional set of the multiple comparisons (Nemenyi method) were performed to find group that were statistically different from others.

Statistical analysis was performed by XLStat software (Addinsoft SARL, New York, NY, USA) in a MS Excel environment (Microsoft Corp., Redmond, WA, USA). Each statistical test in this study was evaluated at the significance level $\alpha = 0.05$.

Results

Table I shows the averages and standard deviations calculated for the whole group of patients and for subgroups divided by treatment position. These values were calculated for total shift in each direction (TS_i) and for every component of the TS_i – full automatic registration ($AR_i^{B,ST}$), automatic registrations based on bone anatomy (AR_i^{B}) and soft tissues (AR_i^{ST}) and for manual corrections (MC_i).

The "Prone" and the "Supine" subgroups were characterized by a normal distribution of each component of the TS_i ($p > 0.05$ for each analysed combination). Moreover, homogeneity of the variances and the absence of statistical differences between averages for these subgroups were confirmed ($p < 0.05$ for each analysed combination). Therefore, the "Prone" and the "Supine" subgroups were merged for further analysis where systematic and random errors and population-based margins were computed for each image guidance protocol.

Table II shows systematic (Σ) and random (σ) errors and population-based margins calculated for every combination of the referencing scheme and IG protocol. In order to evaluate the impact of each combination, corresponding parameters for no image guidance (NIG) scenario were computed. The greatest reduction in systematic and random errors was obtained for protocols IG-2 and IG-3. Margins computed for these protocols were more than two times smaller than margins which should be added on the basis of the NIG scenario. The worst results, which were not significantly different from the results of the NIG scenario, were obtained for IG-4. Analysing the impact of reference schemes, it could be noted that the best results were obtained for the scheme based on the first five fractions (R5) ($p < 0.05$ for each evaluated protocol).

Table I

The averages and standard deviations (in brackets) of the total shift (TS), full automatic registration ($AR^{B,ST}$), automatic registrations based on a bone anatomy (AR^{B}) and soft tissues (AR^{ST}) and manual correction (MC) for each direction (x, y, z), calculated for the whole group of patients and for patients divided by treatment positions (prone and supine).

Direction	Left/right	Superior/inferior	Anterior/posterior
TS [mm]			
Whole group	−0.1 (4.2)	−0.3 (2.8)	0.2 (2.7)
Prone	−0.1 (3.8)	−0.7 (2.9)	0.0 (2.9)
Supine	−0.1 (4.5)	−0.1 (2.6)	0.4 (2.5)
$AR^{B,ST}$ [mm]			
Whole group	0.1 (4.0)	−0.4 (2.9)	0.9 (2.9)
Prone	0.2 (3.7)	−1.0 (3.0)	1.1 (3.3)
Supine	0.0 (4.2)	0.2 (2.8)	0.8 (2.5)
AR^{B} [mm]			
Whole group	0.0 (4.5)	−0.1 (3.3)	0.4 (3.2)
Prone	0.2 (4.2)	−0.2 (3.6)	0.0 (3.4)
Supine	−0.1 (4.8)	0.0 (3.0)	0.7 (3.0)
AR^{ST} [mm]			
Whole group	0.1 (1.1)	−0.3 (1.6)	0.5 (2.1)
Prone	0.1 (1.2)	−0.8 (1.8)	1.1 (2.4)
Supine	0.0 (1.0)	0.2 (1.3)	0.0 (1.8)
MC			
Whole group	−0.2 (1.3)	0.0 (1.5)	−0.7 (2.3)
Prone	−0.3 (1.4)	0.4 (1.5)	−1.1 (2.6)
Supine	−0.1 (1.1)	−0.2 (1.4)	−0.4 (2.0)

Table II

Systematic (Σ) and random (σ) errors and population-based margins in millimetres calculated for no image guidance (NIG) scenario and for each combination of the image guidance (IG) protocol and referencing scheme.

IG protocol	Referencing scheme	Left/right			Superior/inferior			Anterior/posterior		
		Σ	σ	Margin	Σ	σ	Margin	Σ	σ	Margin
NIG		1.9	3.8	7.4	1.7	3.6	6.8	1.7	2.8	6.2
IG-1	R1	0.9	3.3	4.8	1.2	2.9	5.0	1.1	2.6	4.6
	R3	1.2	3.3	5.2	1.1	2.6	4.6	1.3	2.6	5.1
	R5	1.1	3.2	5.0	1.1	2.7	4.6	1.2	2.5	4.8
IG-2	R1	0.6	1.1	2.3	0.6	1.4	2.5	0.9	1.7	3.4
	R3	0.6	1.0	2.2	0.6	1.3	2.3	0.9	1.6	3.3
	R5	0.5	1.0	2.0	0.5	1.2	2.2	0.9	1.5	3.2
IG-3	R1	0.8	1.5	3.1	0.8	1.7	3.2	1.2	1.9	4.3
	R3	0.7	1.5	2.9	0.8	1.8	3.2	1.1	1.9	4.1
	R5	0.7	1.7	3.0	0.7	1.6	3.0	1.1	1.8	4.0
IG-4	R1	1.9	3.6	7.1	1.8	3.3	6.7	1.5	2.6	5.6
	R3	1.8	3.5	6.9	1.8	2.9	6.5	1.5	2.4	5.3
	R5	1.7	3.4	6.7	1.7	2.8	6.3	1.4	2.3	5.2

Table III

Patients divided by failed observations (N) for each combination of the image guidance (IG) protocol and referencing scheme and for no image guidance (NIG) scenario.

IG protocol	Referencing scheme	$N = 0$	$N = 1$	$N = 2$	$N = 3$	$N > 3$
		Number of patients (%)				
NIG		11 (18.3)	13 (21.7)	14 (23.3)	4 (6.7%)	18 (30.0)
IG-1	R1	13 (21.7)	10 (16.7)	15 (25.0)	6 (10.0)	16 (26.7)
	R3	15 (25.0)	11 (18.3)	12 (20.0)	5 (8.3)	17 (28.3)
	R5	17 (28.3)	10 (16.7)	13 (21.7)	4 (6.7)	16 (26.7)
IG-2	R1	23 (38.3)	11 (18.3)	9 (15.0)	4 (6.7)	13 (21.7)
	R3	26 (43.3)	10 (16.7)	10 (16.7)	2 (3.3)	12 (20.0)
	R5	25 (41.7)	12 (20.0)	9 (15.0)	2 (3.3)	12 (20.0)
IG-3	R1	17 (28.3)	13 (21.7)	10 (16.7)	5 (8.3)	15 (25.0)
	R3	19 (31.7)	12 (20.0)	12 (20.0)	3 (5.0)	14 (23.3)
	R5	20 (33.3)	13 (21.7)	11 (18.3)	2 (3.3)	14 (23.3)
IG-4	R1	10 (16.7)	12 (20.0)	11 (18.3)	8 (13.3)	19 (31.7)
	R3	11 (18.3)	13 (21.7)	13 (21.7)	6 (10.0)	17 (28.3)
	R5	12 (20.0)	14 (23.3)	11 (18.3)	6 (10.0)	17 (28.3)

Table III shows the number of patients grouped by N: the third column ($N = 0$) includes patients for whom shifts were always smaller than the applied margins; fourth column ($N = 1$) includes patients for whom one or more of the shifts recorded during one fraction were higher than the applied margins (one failed observation); the fifth column ($N = 2$) includes patients for whom failed observations were recorded twice; sixth column ($N = 3$) – failed observations were recorded three times and seventh column ($N > 3$) – failed observations were recorded more than three times.

Table IV

Overall time for image guidance procedures performed during 25 fractions of the prostate treatment.

IG protocol	Referencing scheme	Number of treatment fractions proceeded by IG procedures: Full IG	Number of treatment fractions proceeded by IG procedures: Automatic registration	Overall time
Daily IG		25	–	113 min 45 sec
IG-1	R1	1	–	4 min 33 sec
	R3	3	–	13 min 39 sec
	R5	5	–	22 min 45 sec
IG-2	R1	1	24	66 min 33 sec
	R3	3	22	70 min 29 sec
	R5	5	20	74 min 25 sec
IG-3	R1	1	24	66 min 33 sec
	R3	3	22	70 min 29 sec
	R5	5	20	74 min 25 sec
IG-4	R1	–	1	2 min 35 sec
	R3	–	3	7 min 45 sec
	R5	–	5	12 min 55 sec

The average imaging time for the whole prostate region performed in a normal mode was 2 minutes and 23 seconds and it ranged from 2 minutes and 11 seconds to 2 minutes and 56 seconds. The average times needed for automatic registration based on the bone anatomy AR^{B} and full automatic registration $AR^{B,ST}$ were the same (12 seconds, ranged from 11 seconds to 14 seconds). The average time for a manual correction was 1 minute and 58 seconds and ranged from 59 seconds to 5 minutes and 31 seconds. Simulations of the overall time needed for the image guidance procedures based on the average of each component, for 25 fractions of the prostate treatment are shown in Table IV.

Discussion

For prostate IMRT, selecting the appropriate IG protocol can reduce the probability of a geographic miss when tight margins are used. However, IG procedures increase the additional radiation dose for imaging, the time of the treatment fraction and, as a result, total time spend by patient in a therapeutic bunker, which is needed to accomplish full dose during the course of the radiation therapy.

Therefore, in this study, we investigated the trade-off between the time consumption of the treatment and the possibility of reducing the margins and, hence, reducing high doses in the organ at risks for four IG protocols that use: (i) a limited number of imaging sessions, IG-1, (ii) reduced registration tasks during daily imaging, IG-2, or (iii) and (iv) mixed methods of the imaging, IG-3 and IG-4.

Our previous study confirmed the absence of statistical differences between the TS_i collected for the groups of patients

treated in supine and prone positions (13). Consequently, for IG-1 we merge these groups and analyze them as a single homogeneous group. For IG-2, IG-3 and IG-4, components of the TS_i were used for calculations of the residual fraction errors (Table I). Therefore, the possibility of merging the "Supine" and "Prone" groups for these protocols was confirmed by the analysis of the normality (Shapiro-Wilk test). The homogeneity of the variance (F-test) and similarity of the central tendency (two-tailed t-Student test for independent samples) were performed according to the recipe presented by us in a previous study (31).

Evaluating the margins calculated for the particular IG protocols we can conclude that the referencing scenario which is based on the first five fractions (R5) is the most appropriate one. The R5 scenario provides the highest reduction of margins for each IG protocol evaluated in this study (Table II). Moreover, a calculated margin based on the R5 scenario provides the best minimisation of failed observations detected for the patients during the course of the radiation therapy (Table III).

A reduced IG strategy (IG-1) is effective in correcting the systematic component of set-up error (8), which makes a greater contribution to the calculation of treatment margin than the random component (28). For example, the margins provided by the IG-1(R5) protocol were 5 mm, 4.6 mm and 4.8 mm in the LR, SI and AP direction, whereas the margins calculated on the basis of the daily IG registration and added to the NIG protocol were 7.4 mm, 6.8 mm and 6.2 mm, respectively (Table II).

Sources of systematic errors are the differences in anatomy between simulation and treatment, and the differences in patient position due to mechanical differences between the simulator and the treatment unit. Examples of random errors include variations in daily alignment to set-up tattoos using in-room lasers and variable prostate position due to inter-fraction changes in rectum and bladder filling (32-35).

To reduce the random error, image guidance should be provided by every fraction of the course of the radiation therapy. However, the daily IG procedure including full registration tasks such as automatic registration followed by manual correction based on visual inspection, constitute a time consuming procedure. The average time needed for daily IG procedures was 113 minutes and 45 seconds in the analysed group of patients (Table IV). The biggest component of the time needed for the full registration procedure is that dedicated to manual correction. Therefore, to speed up the daily registration procedure the IG-2 protocol was designated. The IG-2 is based on daily shifts collected by the automatic registration using the "Bone and Soft Tissue" technique and the margins were calculated on the basis of manual correction not included in the daily correction of the patient position but still followed by quick visual check to exclude large errors of the positioning caused by some potential fails of the software used for the registration (Figure 1). As a result, the time needed for full image guidance procedures during the whole course of the radiation therapy according to the IG-2 protocol was almost twice shorter than for daily IG procedures, including full registration tasks (*e.g.* 113 minutes and 45 seconds for daily, full IG versus 74 minutes and 25 seconds for IG-2(R5) protocol). Moreover, in comparison to the IG-1, the daily automatic registration provided by the IG-2, effectively reduces random errors and allows to calculate the margins on the basis of residual errors caused by manual correction. For example, the margins for IG-1(R5) and for IG-2(R5) were: 5 mm, 4.6 mm and 4.8 mm for the LR, SI and AP direction for IG-1(R5) and 2 mm, 2.2 mm and 3.2 mm for the LR, SI and AP direction for IG-2(R5) (Table II). Clearly, the time needed for image guidance according to the IG-1 is almost 1 hour shorter than for the IG-2 (Table IV). This effect was caused by the fact that the IG-2 protocol included the scanning procedures performed daily for each fraction of the radiation therapy course and for the IG-1 protocol, the number of scanning procedures was reduced only to the number of the first fractions which were used as a reference (R1, R3 or R5). These two types of IG protocols should be carefully considered before the beginning of the treatment. On the one hand, the first of them (IG-1), in comparison to the second (IG-2), allows for a reduction in both the time needed for the image guidance procedures and in the team effort which is necessary during daily automatic registration. However, the IG-1 is more dependent on random errors, which are effectively reduced by the IG-2. Higher accuracy of the patient-dependent margins followed by the IG-2 protocol was showed in Table III. It should be noted that smaller margins provided by the IG-2 are obtained at the cost of higher imaging dose as compared with the IG-1. Shah *et al.* (36) showed that the imaging session performed for the prostate region in the normal mode on the helical tomotherapy deliver 1 cGy additional dose. Therefore, we estimate that the imaging dose for the IG-1(R5) was 5 times lower than that for the IG-2(R5), and was 5 cGy for the IG-1(R5) and 25 cGy for the IG-2(R5), respectively.

The third type of the IG protocol evaluated in this study implies automatic registration for the rest of the fractions using the "Bone" technique (Figure 1). Results of the automatic registration based on the bone anatomy obtained from the MVCT and CT studies are comparable with the results from registrations performed on the digitally reconstructed radiographs with MV or kV two-dimensional imaging without markers (portal imaging). Thus, the IG-3 could simulate a scenario for conventional accelerators (*e.g.* Varian, Electa) when for initial k fractions cone-beam CT studies were performed and portal imaging controlled the rest of the

n-k fractions. The margins calculated according to the IG-3 were placed between the higher IG-1 margins and the lower IG-2 margins (Table II). Moreover, worse result in terms of the accuracy of the calculated margins is observed for the IG-3 than for the IG-2 (Table III). It is due to the fact that the IG-3 uses less accurate methods of image registration for the remaining *n-k* fractions than the IG-2 ("Bone" technique against the "Bone and Soft Tissue" technique). However, the IG-3 protocol is still interesting to the potential investigation because it provides better results for the reduction of the margin and its accuracy than the IG-1 (Tables II and III).

The last protocol (IG-4), assumes that the margins were calculated from residual errors caused from the difference between the total shifts, and the average shifts obtained from the automatic registrations based on the bony anatomy, and which were performed during a few first fractions (R1, R3 or R5) (Figure 1). On the conventional linac it should be described as a control by the portal imaging (7). Initial k fractions for the IG-4 protocol were biased by the lack of information about the shifts, which should be added for these fractions and which result from automatic registration of the soft tissues (AR_i^{ST}) and manual corrections (MC_i). The result obtained for the IG-4 does not decrease the calculated margins nor increases its accuracy in correspondence to the NIG scheme (Tables II and III). Therefore we do not recommend it as a protocol to be used to increase the conformity of the dose caused in a direct way by the image guidance procedures.

Conclusion

The IG-4 based on the bone anatomy registrations is not recommended as a protocol to be used to increase the conformity of the dose. The choice between the IG-1 using a limited number of imaging sessions, the IG-2 based on the reduced registration tasks during daily imaging or the IG-3 simulating the scheme when cone-beam CT for the initial fractions is followed by portal imaging for the rest of the fractions should be validated in the context of: (i) institutional practice regarding patient set-up procedure and its time consumption, (ii) the acceptable balance between the amount of dose delivered to the organ at risk and the additional imaging dose and (iii) patient anatomical conditions, directly influencing the random errors, which could decrease the accuracy of the delivered dose.

If the additional time needed for image-guidance and additional imaging dose is acceptable, we recommend the IG-2, which reduced random errors more effectively than the IG-1 while providing a shorter time needed for set-up than full image guidance performed in the daily scheme.

Declaration of Conflict of Interest

Nothing to declare.

References

1. Milecki P, Piotrowski T & Dymnicka M. The comparison of radiotherapy techniques for treatment of the prostate cancer: the three-field vs. the four-field. *Neoplasma 51*, 64-69 (2004).
2. Leszczyński W, Ślosarek K & Szlag M. Comparison of dose distribution in IMRT and RapidArc technique in prostate radiotherapy. *Rep Pract Oncol Radiother 17*, 347-351 (2012). DOI: 10.1016/j.rpor.2012.05.002
3. Korreman S, Rasch C, McNair H, Verellen D, Oelfke U, Maingon P, *et al.* The European society of therapeutic radiology and oncology – European Institute of radiotherapy (ESTRO-EIR) report on 3D CT-based in-room image guidance systems: a practical and technical review and guide. *Radiother Oncol 94*, 129-144 (2010). DOI: 10.1016/j.radonc.2010.01.004
4. Malicki J. The importance of accurate treatment planning, delivery, and dose verification. *Rep Pract Oncol Radiother 17*, 63-65 (2012). DOI: 10.1016/j.rpor.2012.02.001
5. Thwaites DI & Malicki J. Physics and technology in ESTRO and in radiotherapy and oncology: past, present and into the 4th dimension. *Radiother Oncol 100*, 327-332 (2011). DOI: 10.1016/j.radonc.2011.09.014
6. Bidmead M, Coffey M, Crellin A, Dobbs J, Driver D, Greener A, *et al. Geometric Uncertainties in Radiotherapy: Defining the Planning Target Volume.* British Institute of Radiology, London (2003).
7. The Royal College of Radiologists, Society and College of Radiographers, Institute of Physics and Engineering in Medicine: *On Target: Ensuring Geometric Accuracy in Radiotherapy*. The Royal College of Radiologists, London (2008).
8. Kupelian PA, Lee C, Langen KM, Zeidan OA, Manon RR, Willoughby TR, *et al.* Evaluation of image-guidance strategies in the treatment of localized prostate cancer. *Int J Radiat Oncol Biol Phys 70*, 1151-1157 (2008). DOI: 10.1016/j.ijrobp.2007.07.2371
9. Meeks S, Kupelian PA, Lee C, Willoughby T, Zeidan O & Langen K. Does image guidance need to be performed daily in the treatment of localized prostate cancers? Implications on treatment margins. *Int J Radiat Oncol Biol Phys 69*, S82-83 (2007). DOI: 10.1016/j.ijrobp.2007.07.149
10. Beldjoudi G, Yartsev S, Battista JJ & van Dyk J. Optimisation of MVCT imaging schedule in prostate cancer treatment using helical tomotherapy. *Cancer Radiother 12*, 316-322 (2008). DOI: 10.1016/j.canrad.2008.03.002
11. Beldjoudi G, Yartsev S, Bauman G, Battista J & van Dyk J. Schedule for CT image guidance in treating prostate cancer with helical tomotherapy. *Br J Radiol 83*, 241-251 (2010). DOI: 10.1259/bjr/28706108
12. Yeung TPC, Yartsev S, Rodrigues G & Bauman G. Evaluation of image-guidance strategies with helical tomotherapy for localized prostate cancer. *J Med Imaging Radiat Oncol 55*, 220-228 (2011). DOI: 10.1111/j.1754-9485.2011.02255.x
13. Bajon T, Piotrowski T, Antczak A, Bak B, Błasiak B & Kaźmierska J. Comparison of dose volume histograms for supine and prone position in patients irradiated for prostate cancer – A preliminary study. *Rep Pract Oncol Radiother 16*, 65-70 (2011). DOI: 10.1016/j.rpor.2011.01.003
14. McIlwraith KA & Blyth C. A study of the effect on accuracy of the introduction of a bellyboard as an immobilisation device to the radical radiotherapy treatment of prostate cancer patients. *J Radiother Pract 11*, 162-169 (2012). DOI: 10.1017/S1460396911000276
15. Mocna M & Zwierzchowski G. Dosimetric verification of the dose calculation algorithms in real time prostate brachytherapy. *Rep Pract Oncol Radiother 13*, 275-279 (2008). DOI: 10.1016/S1507-1367(10)60013-2
16. Kanikowski M, Skowronek J, Kubaszewska M, Chicheł A & Milecki P. Permanent implants in treatment of prostate cancer. *Rep*

Pract Oncol Radiother 13, 150-167 (2008). DOI: 10.1016/S1507-1367(10)60006-5
17. Kanikowski M, Skowronek J & Chicheł A. HDR brachytherapy of prostate cancer – two years experience in greater poland cancer centre. *J Contemp Brachyther 1*, 137-144 (2009).
18. International Commission on Radiation Units and Measurements. ICRU report 83: Prescribing, recording, and reporting photon beam intensity-modulated radiation therapy (IMRT). *Journal of the ICRU 10*, NP (2010). DOI: 10.1093/jicru/ndq001-013
19. Skórska M & Piotrowski T. Optimization of treatment planning parameters used in tomotherapy for prostate cancer patients. *Physica Medica 29*, In Press (2013). DOI: 10.1016/j.ejmp.2012.03.007
20. Skórska M & Piotrowski T. Empirical estimation of beam-on time for prostate cancer patients treated on Tomotherapy. *Rep Pract Oncol Radiother 18*, In Press (2013). DOI: 10.1016/j.rpor.2012.12.005
21. Ruchala KJ, Olivera GH & Kapatoes JM. Limited-data image registration for radiotherapy positioning and verification. *Int J Radiat Oncol Biol Phys 54*, 592-605 (2002). DOI: 10.1016/S0360-3016(02)02895-X
22. Rivest D, Riauka T, Murtha A & Fallone B. Dosimetric implications of two registration based patient positioning methods in prostate image guided radiation therapy (IGRT). *Radiol Oncol 43*, 203-212 (2009). DOI: 10.2478/v10019-009-0030-z
23. Adamczyk M, Piotrowski T & Adamiak E. Evaluation of combining bony anatomy and soft tissue position correction strategies for IMRT prostate cancer patients. *Rep Pract Oncol Radiother 17*, 104-109 (2012). DOI: 10.1016/j.rpor.2012.01.005
24. Snir JA, Battista JJ, Bauman G & Yartsev S. Evaluation of interfraction prostate motion using kilovoltage cone beam computed tomography during radiotherapy. *Clinical Oncology 23*, 625-631 (2011). DOI: 10.1016/j.clon.2011.03.007
25. de Boer HC & Heijmen BJ. A protocol for the reduction of systematic patient setup errors with minimal portal imaging workload. *Int J Radiat Oncol Biol Phys 50*, 1350-1365 (2001). DOI: 10.1016/S0360-3016(01)01624-8
26. Bortfeld T, van Herk M & Jiang SB. When should systematic patient positioning errors in radiotherapy be corrected? *Phys Med Biol 47*, 297-302 (2002). DOI: 10.1088/0031-9155/47/23/401
27. Broggi S, Cozzarini C, Fiorino C, Maggiulli E, Alongi F, Cattaneo GM, *et al.* Modeling set-up error by daily MVCT for prostate adjuvant treatment delivered in 20 fractions: Implications for the assessment of the optimal correction strategies. *Radiother Oncol 93*, 246-252 (2009). DOI: 10.1016/j.radonc.2009.08.029
28. van Herk M, Remeijer P, Rasch C & Lebesque JV. The probability of correct target dosage: dose-population histograms for deriving treatment margins in radiotherapy. *Int J Radiat Oncol Biol Phys 47*, 1121-1135 (2000). DOI: 10.1016/S0360-3016(00)00518-6
29. Ryczkowski A & Piotrowski T. Tomotherapy archive structure and new software tool for loading and advanced analysis of data contained in it. *Rep Pract Oncol Radiother 16*, 58-64 (2011). DOI: 10.1016/j.rpor.2011.01.004
30. Piotrowski T, Bak B, Kazmierska J, Skorska M & Ryczkowski A. Tomotherapy: Implications on daily workload and scheduling patients based on three years experience. *Int J Radiat Oncol Biol Phys 84*, S773 (2012). DOI: 10.1016/j.ijrobp.2012.07.2068
31. Piotrowski T, Yartsev S, Rodrigues G & Bajon T. Comparative analysis of image guidance in two institutions for prostate cancer patients. *Radiother Oncol 103*, S559 (2012). DOI: 10.1016/S0167-8140(12)71797-8
32. Pinkawa M, Asadpour B, Siluschek J, Gagel B, Piroth MD, Demirel C, *et al.* Bladder extension variability during pelvic external beam radiotherapy with a full or empty bladder. *Radiother Oncol 83*, 163-167 (2007). DOI: 10.1016/j.radonc.2007.03.015
33. Fiorino C, Di Muzio N, Broggi S, Cozzarini C, Maggiulli E, Alongi F, *et al.* Evidence of limited motion of the prostate by carefully emptying the rectum as assessed by daily MVCT image guidance with helical tomotherapy. *Int J Radiat Oncol Biol Phys 71*, 611-617 (2008). DOI: 10.1016/j.ijrobp.2008.01.048
34. Engels B, Tournel K, Soete G & Storme G. Assessment of rectal distention in radiotherapy of prostate cancer using daily megavoltage CT image guidance. *Radiother Oncol 90*, 377-381 (2009). DOI: 10.1016/j.radonc.2008.12.005
35. Paluska P, Hanus J, Sefrova J, Rouskova L, Grepl J, Jansa J, *et al.* Utilization of cone-beam CT for offline evaluation of target volume coverage during prostate image-guided radiotherapy based on bony anatomy alignment. *Rep Pract Oncol Radiother 17*, 134-140 (2012). DOI: 10.1016/j.rpor.2012.03.003
36. Shah AP, Langen KM, Ruchala KJ, Cox A, Kupelian PA & Meeks SL. Patient dose from megavoltage computed tomography imaging. *Int J Radiat Oncol Biol Phys 70*, 1579-1587 (2008). DOI: 10.1016/j.ijrobp.2007.11.048

Received: February 9, 2013; Revised: March 7, 2013; Accepted: March 11, 2013